J. Makita, C. Sundahl, G. Ciovati, C. B. Eom, and A. Gurevich, Phys. Rev. Res. **4**, 013156 (2022)

Nonlinear Meissner effect in Nb_3Sn coplanar resonators

Junki Makita

Superconducting Radio Frequency (SRF) Cavities

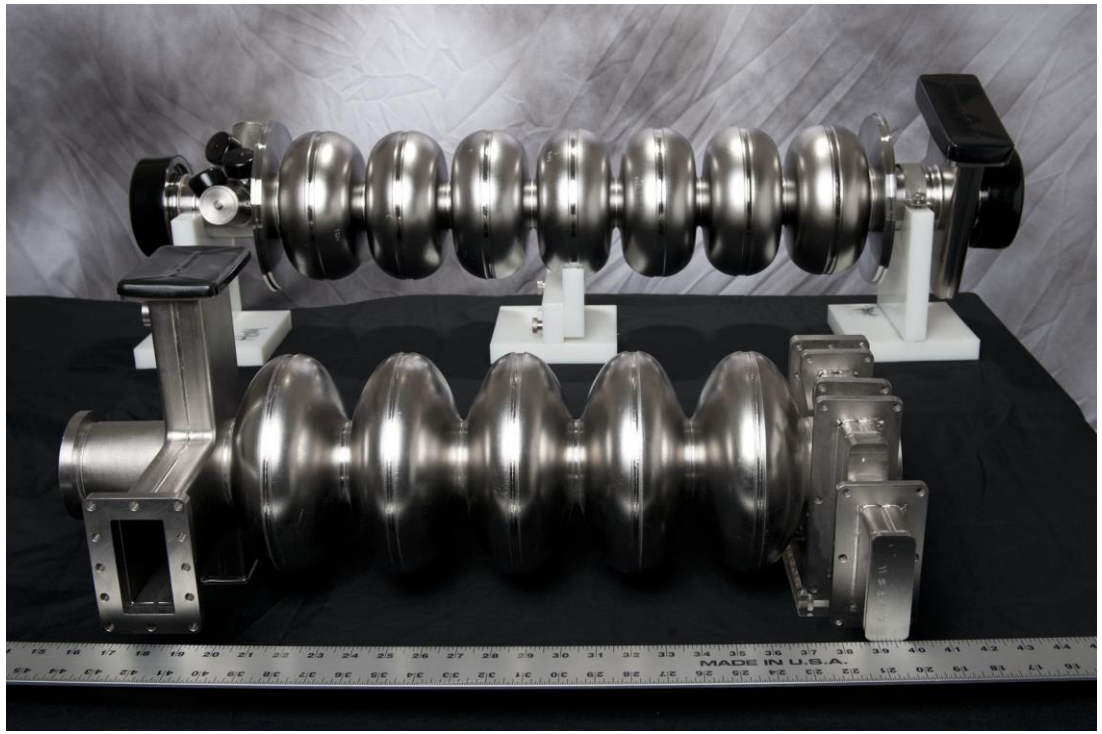

- Nb cavities are operated at 2K
- Nb cavities are approaching the intrinsic limit of the material
- Look for alternative materials for further improvement
- Nb_3Sn is the most promising alternative so far

Nb_3Sn

- Critical Temperature ~ 18 K
  - Increase the operating temperature from 2K to $\sim$ 4K while maintaining high Q_0
  - Reduces the cryogenic operation cost and the size of the plant
  - Opens up the possibility for the operation with LHe free cryocooler
- High superheating field
  - Cavity can sustain a higher magnetic field than Niobium
  - Higher maximum accelerating field up to 100MV/m, twice that of Nb
- Current state-of-the-art Nb_3Sn cavities can reach $\sim$20 MV/m

C. Sundahl, et al., Sci. Rep. **11**, 7770 (2021).

Nb_3Sn thin film study

- Study the response of Nb_3Sn thin-film resonator as a function of magnetic field
- Film was grown by Chris Sundahl from the University of Wisconsin-Madison.
- Co-sputtered using Sn and Nb Targets

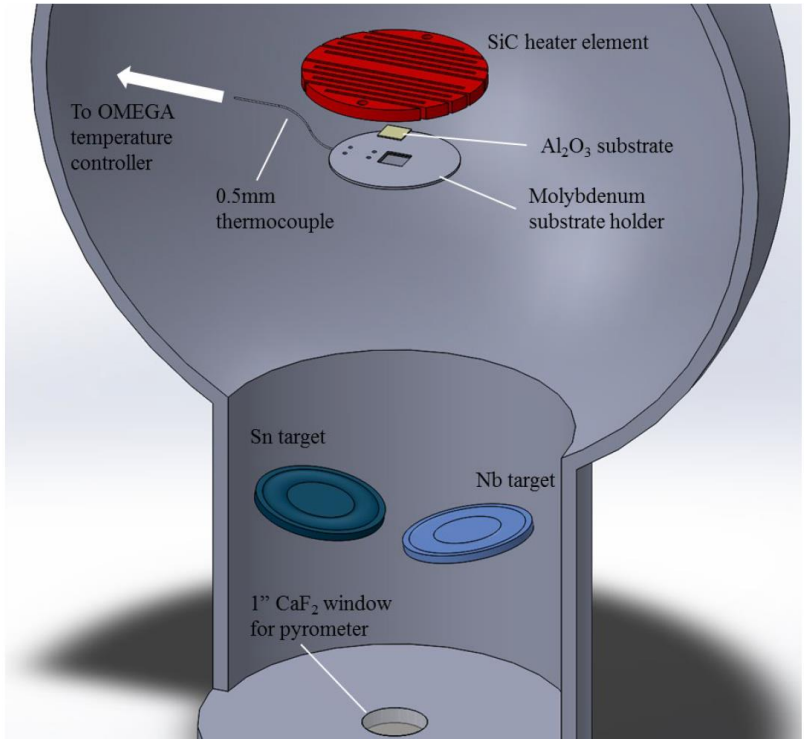

Tc and Surface Topography

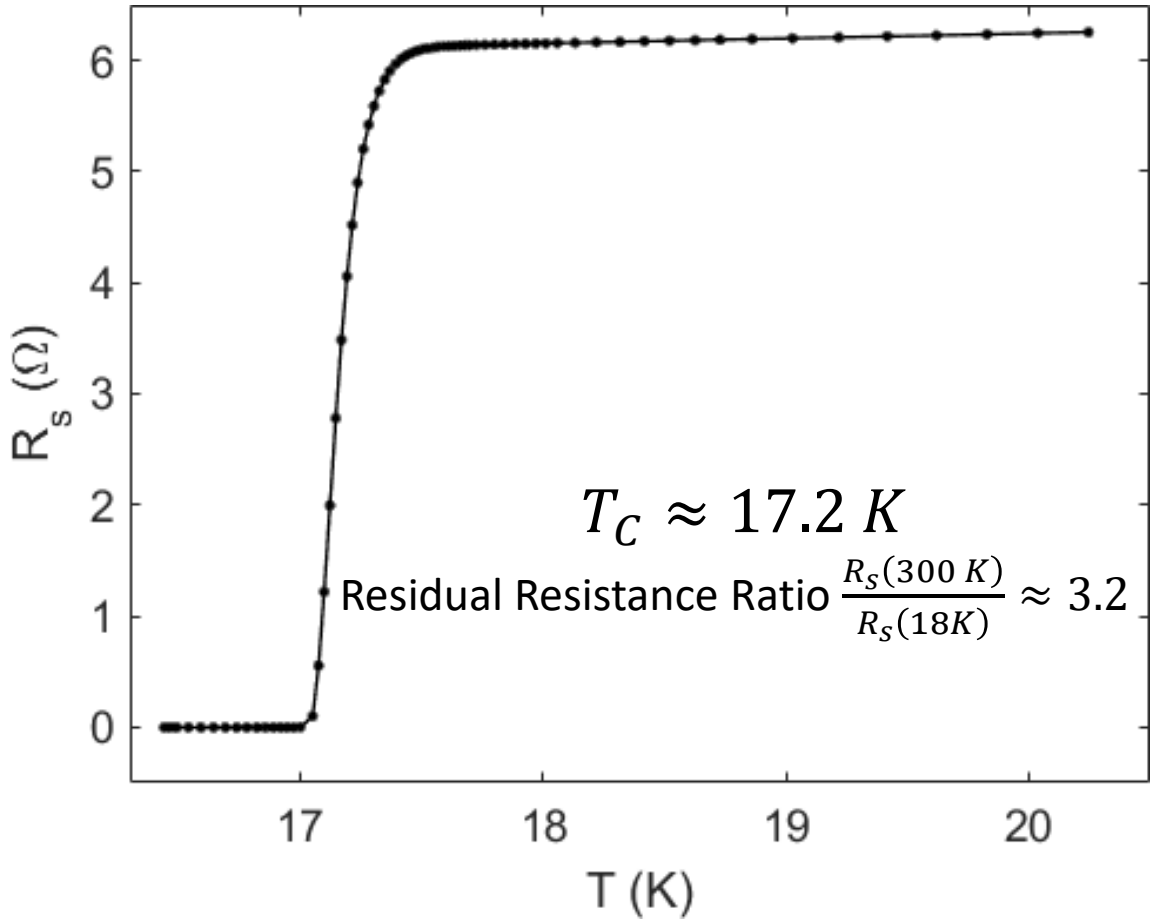

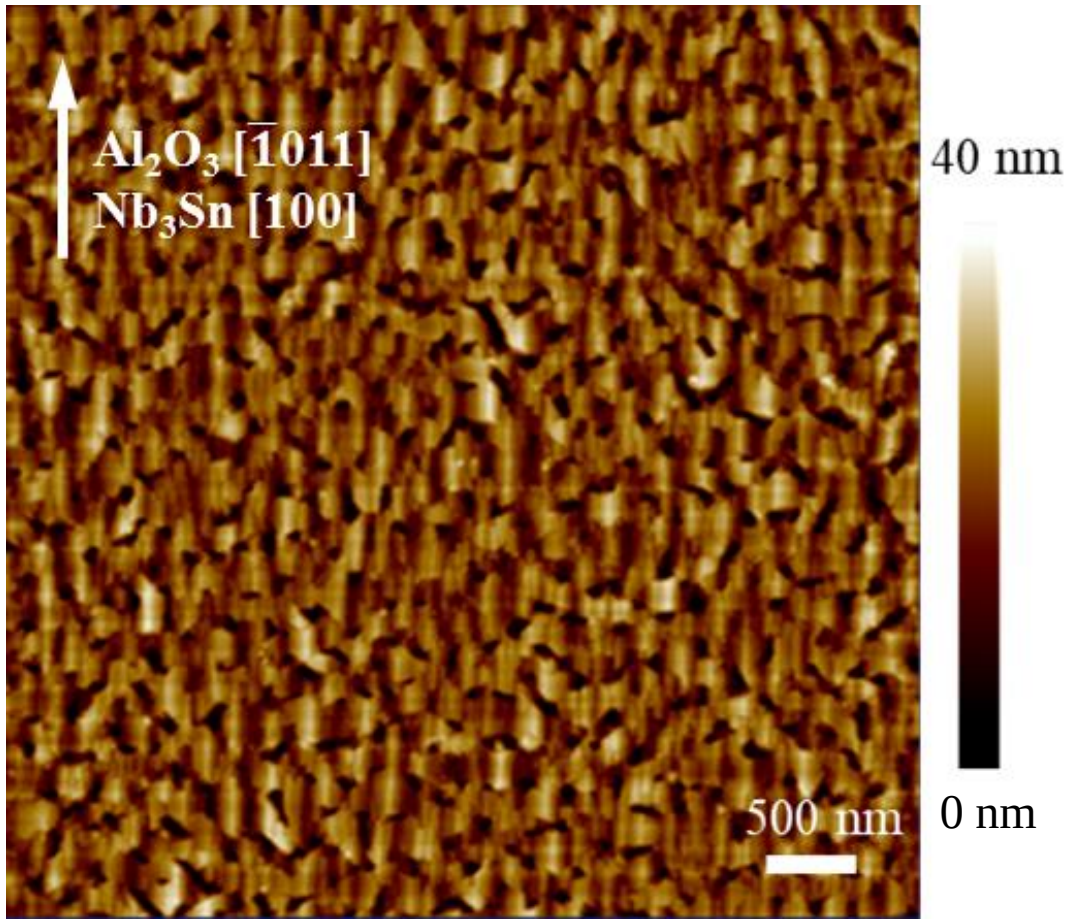

Meissner effect (Linear)

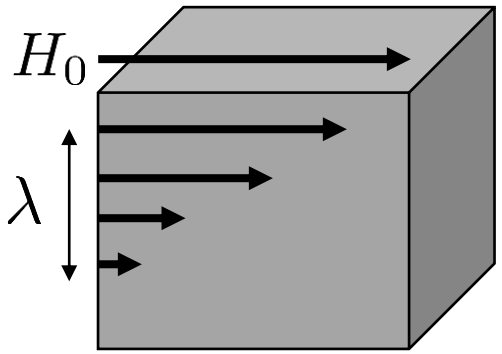

$$\mathbf{H}(z) = H_0 e^{-z/\lambda}$$

$$\mathbf{J}(z) = \frac{H_0}{\lambda} e^{-z/\lambda}$$

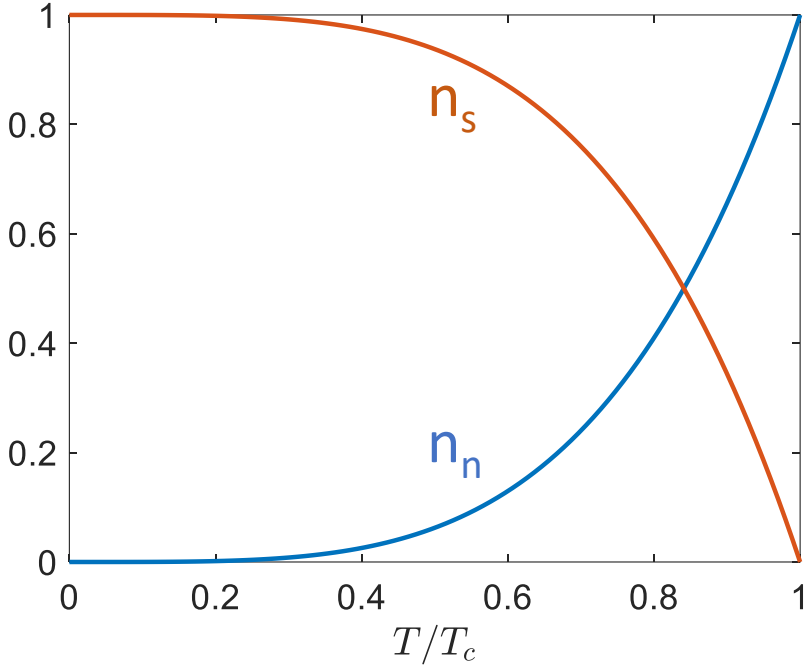

Two-fluid model: $n(T) = n_s(T) + n_n(T)$

$$\frac{d\mathbf{J_s}}{dt} = \frac{e^2 n_s}{m}\mathbf{E}$$ First London Equation

$$\lambda^2 \nabla \mathbf{H} - \mathbf{H} = 0$$ Second London Equation

(Using $\nabla \times \mathbf{E} = -\mu_0 \partial_t \mathbf{B}$ and $\nabla \times \mathbf{H} = \mathbf{J}_s$)

$$\boxed{\lambda(T) = \left(\frac{m}{e^2 n_s(T)\mu_0}\right)^{1/2}}$$

Nonlinear Meissner Effect (NLME)

$$\mathbf{J} = -\frac{\mathbf{A}}{\mu_0 \lambda^2} \qquad \lambda = \left(\frac{m}{e^2 n_s \mu_0}\right)^{1/2}$$

- Any dependence on λ on the current density results in the nonlinear Meissner effect
- Possible Causes:
  - Pair breaking effect in which the strong field reduces n_s
  - Weakly coupled grain boundaries and local non-stoichiometry on the surface cause an additional increase in λ
- Important for Nb_3Sn coated SRF cavity because it can introduce nonlinear response to surface impedance.

Probing NLME

- We probed NLME by measuring the reactive part of the surface impedance $Z = R_S + iX_S$
- Reactive part → Kinetic Inductance

$$\frac{1}{2}L_k I^2 = \frac{1}{2}\int \mu\lambda^2 |\mathbf{J}|^2 dS$$

- For a rectangular strip with thickness $t \ll \lambda$ and width w

$$L_k = \frac{\mu\lambda^2}{wt}$$

- Resonant frequency of the resonator: $f_r = \frac{1}{2\pi\sqrt{LC}} = \frac{1}{2\pi\sqrt{(L_g + L_k)C}}$

Nb3Sn Coplanar Waveguide Resonator

- Transmission line resonator pattern on a thin film Nb_3Sn
- Measure the resonant frequency as a function of the field to probe the change in kinetic inductance
- Study the dependence on the field orientation
- B || z : parallel to the rf current
- B || y : perpendicular to the rf current

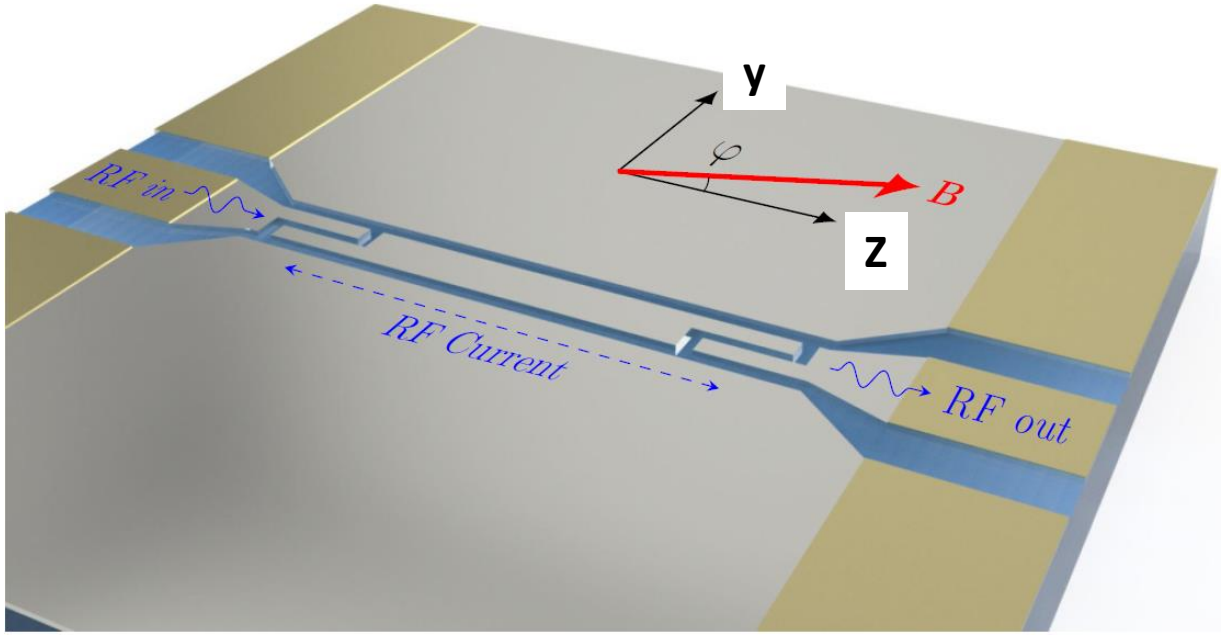

Sample Design

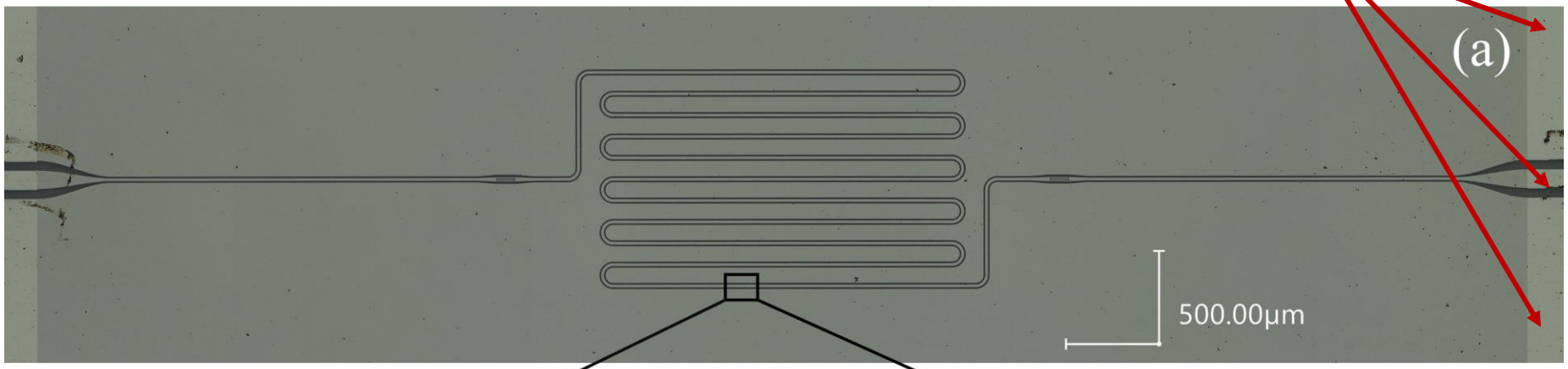

Pd landing pads

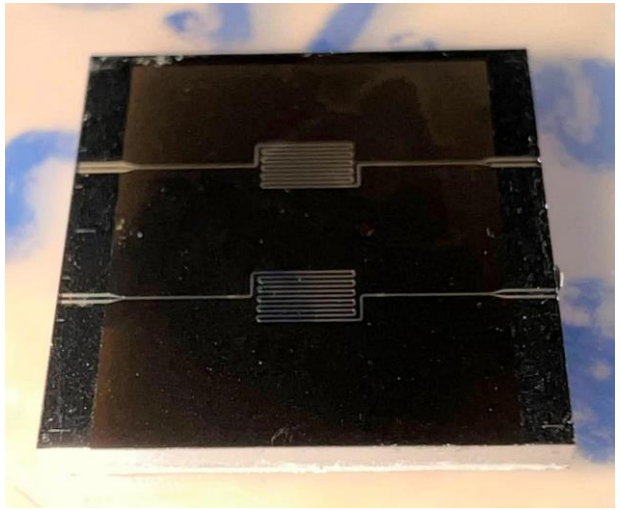

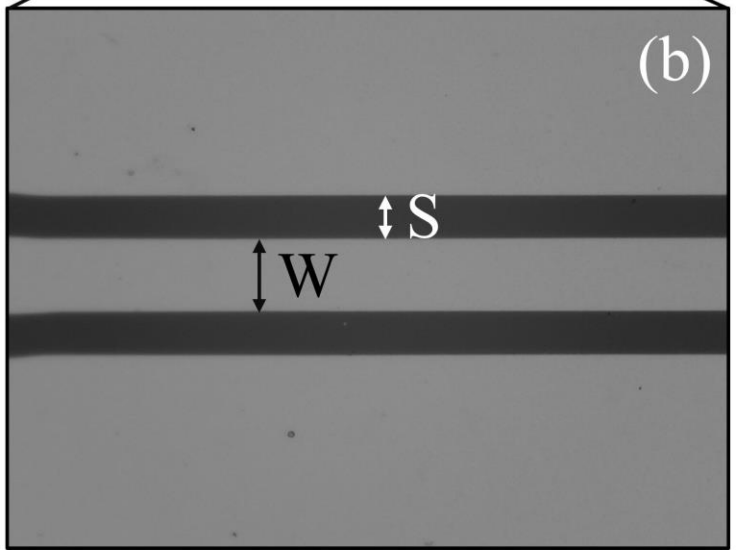

- $w = 14.90\ \mu m, s = 8.86\ \mu m$
- Total length: 24.6mm (2.236GHz)
- Deposited on 10mm x 10mm Al_2O_3
- Using $t = 50nm \ll \lambda$ film increases the onset of penetration of the magnetic fluxes in the material

Vortex state

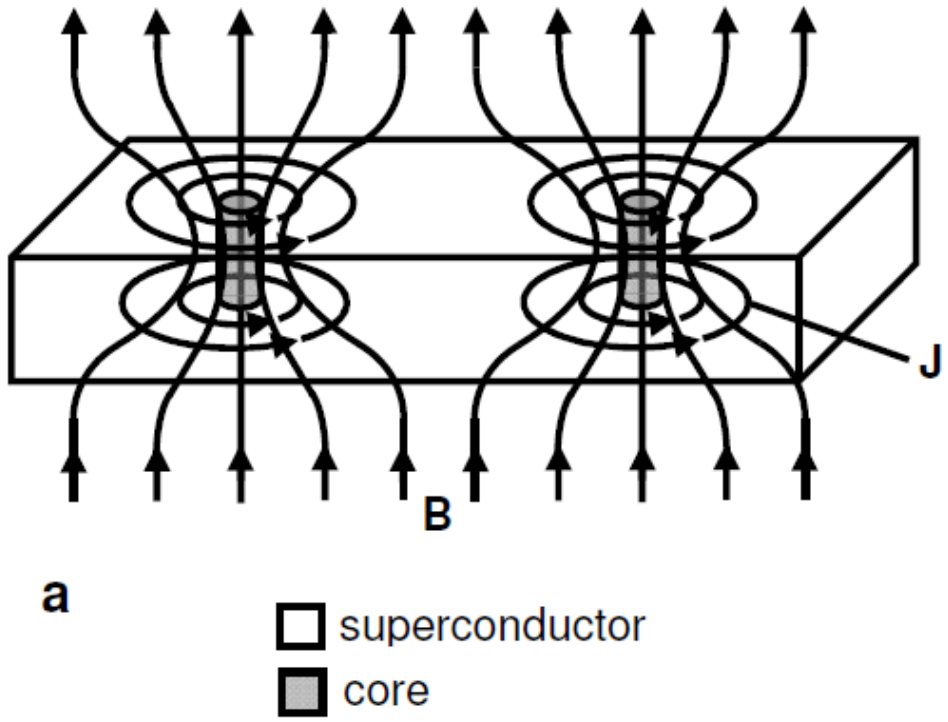

- In type II superconductor, when $B > B_{c1}$ it becomes energetically favorable for the flux to penetrate the material as vortices.
- n_s drops to zero at the core
- We want to avoid vortices to probe NLME

$$B_{c1} = \frac{2\phi_0}{\pi t^2} \ln\left(\frac{t}{\xi}\right) \approx 1.2\,\mathrm{T}$$

(Almost 2x bulk value)

Probe Station

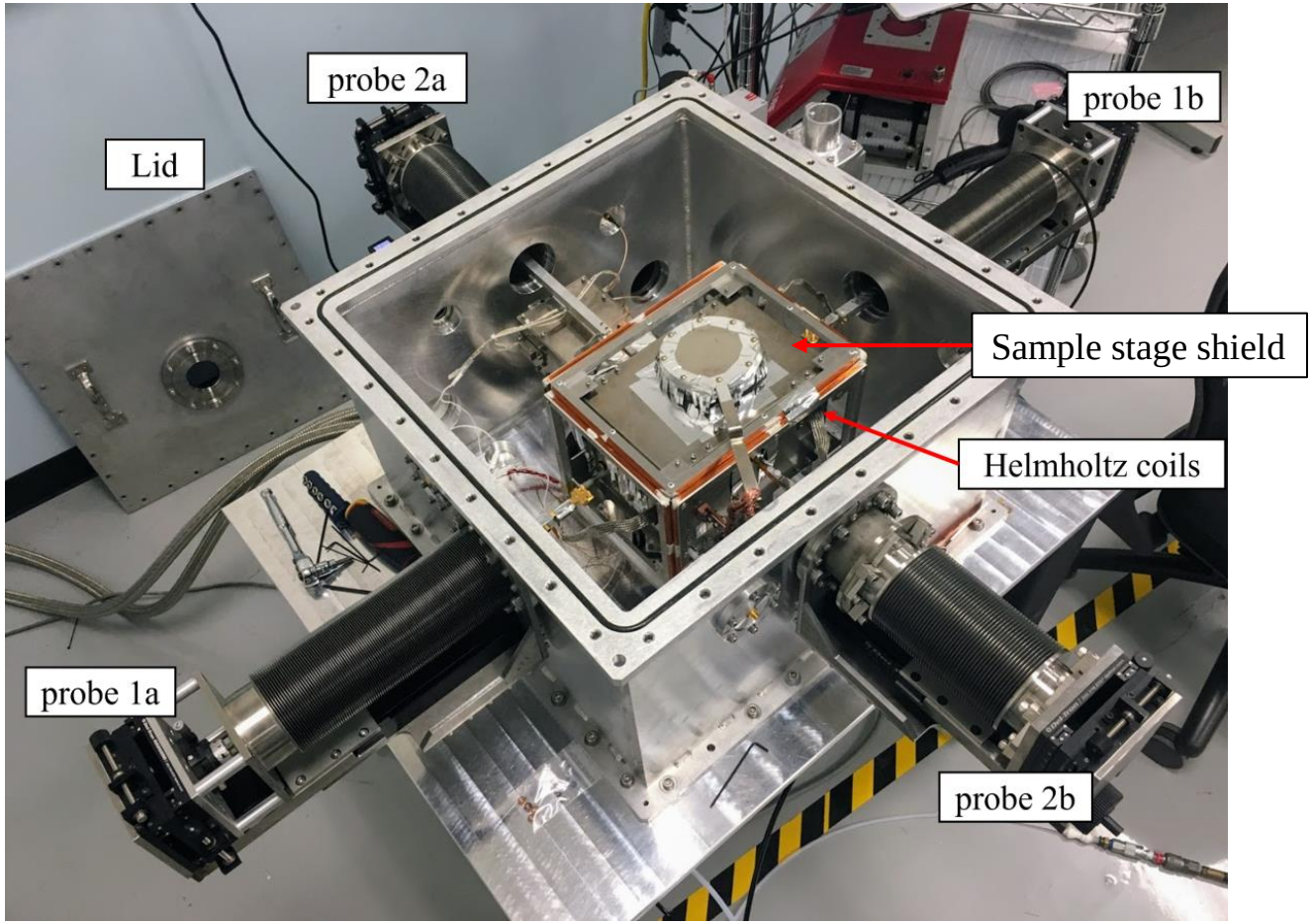

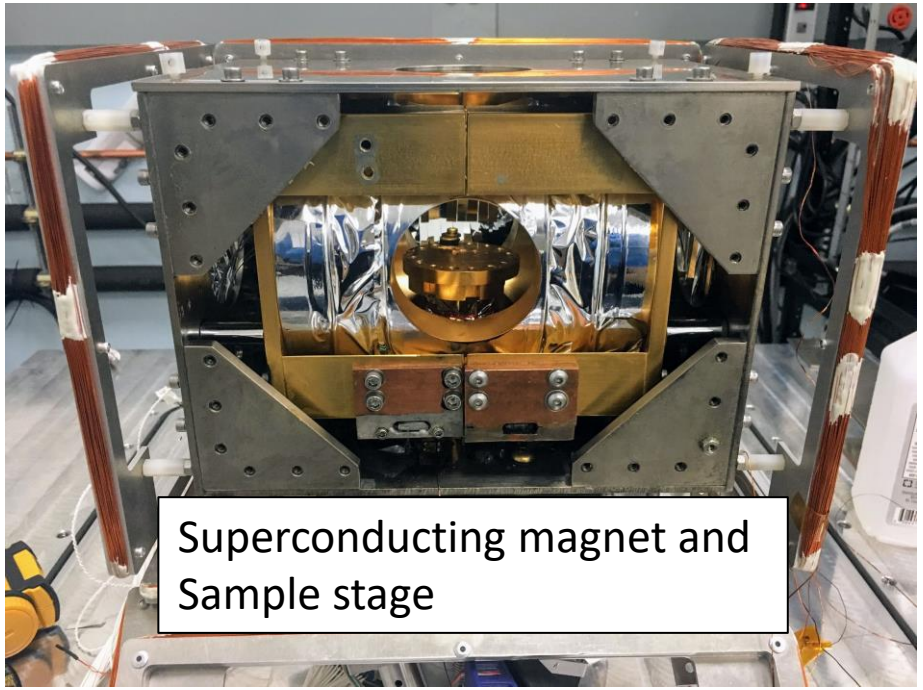

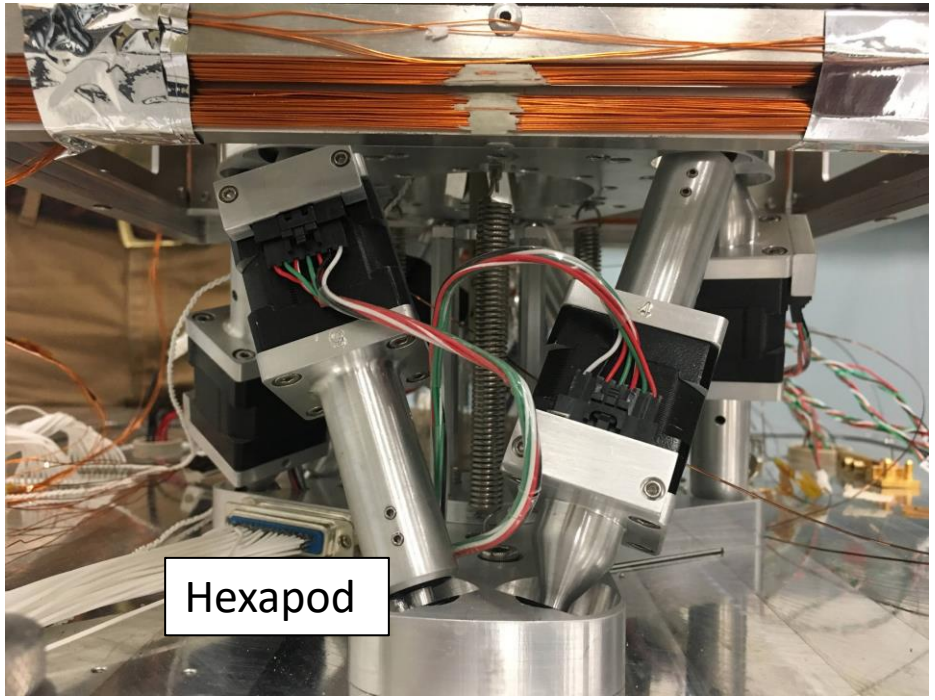

Probe Station Sample stage

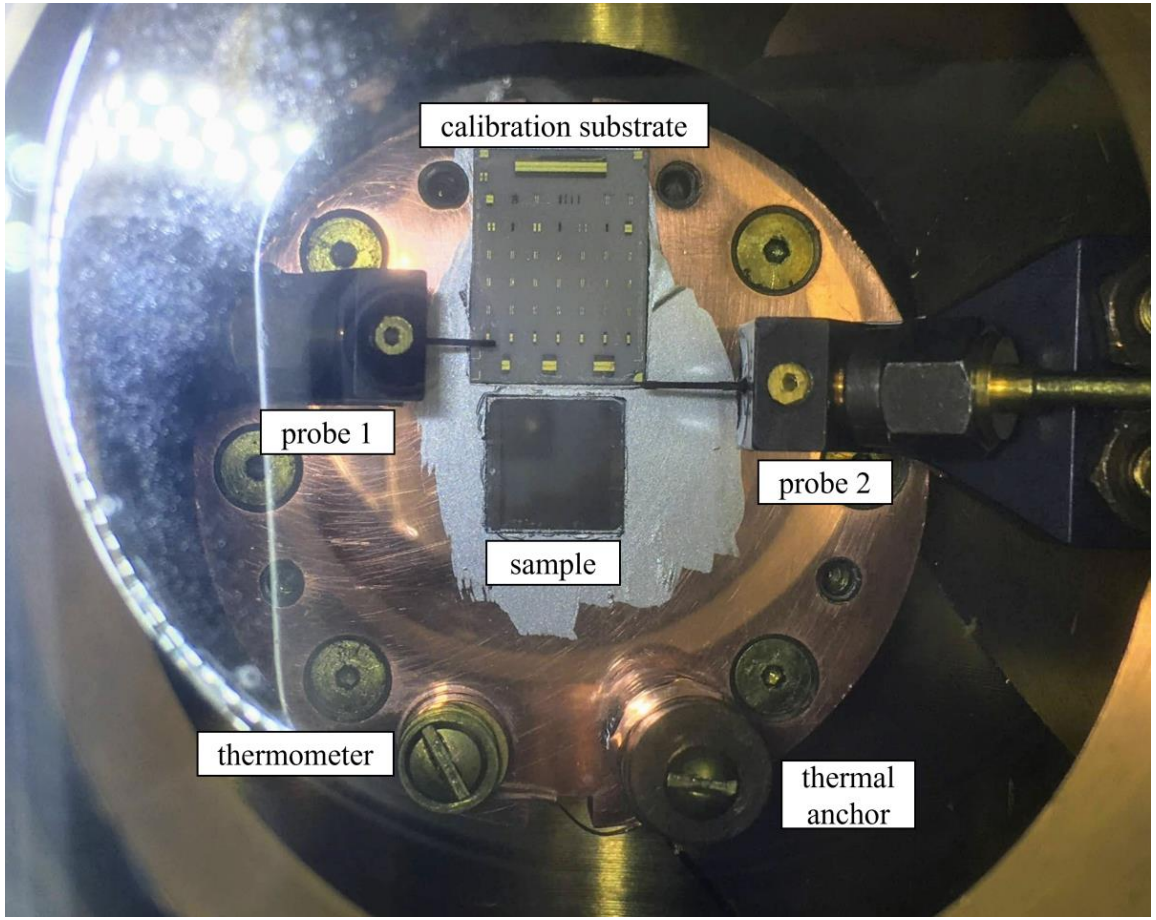

Top view of the sample stage

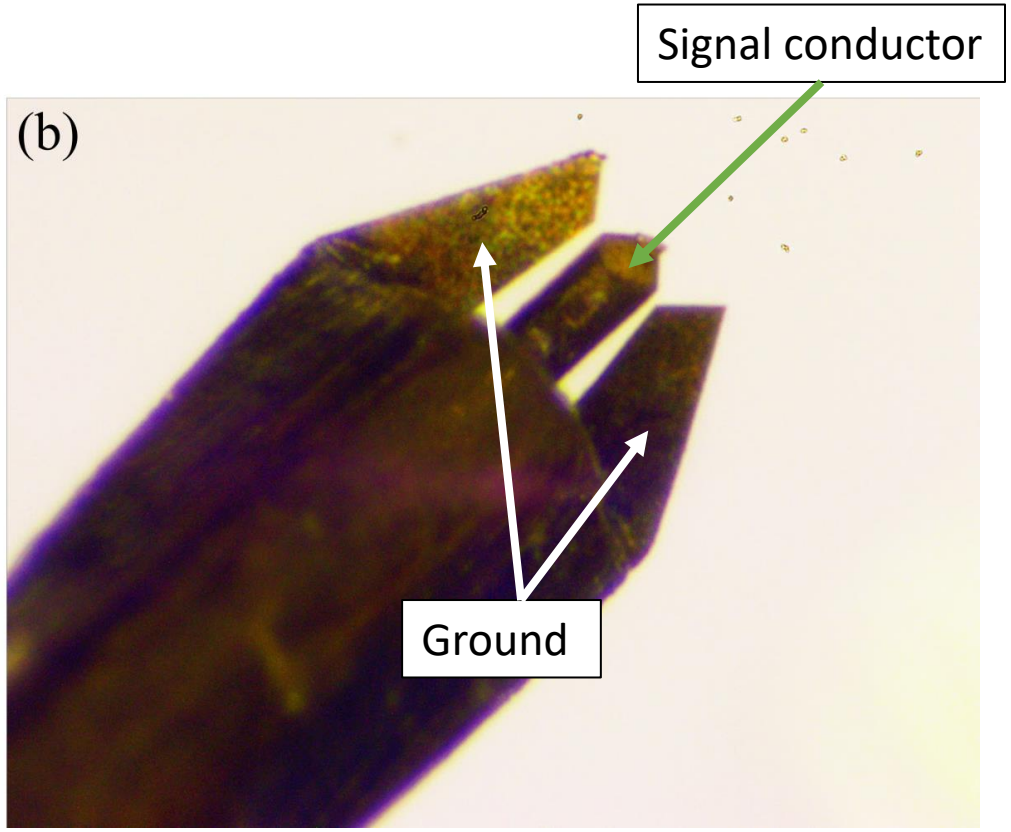

Probe tips

Experimental Procedure

- Cool down the sample to 7K
- Measure the resonant frequency f_r as a function of T to calculate $\lambda(T)$
- Align the field to be parallel to the surface of the film
- Measure the shift in $f_r(B)$ as a function of the field in two orientations: $B \parallel z$ and $B \parallel y$.
- Repeat for higher temperatures up to 12K.

Resonant frequency vs Temperature

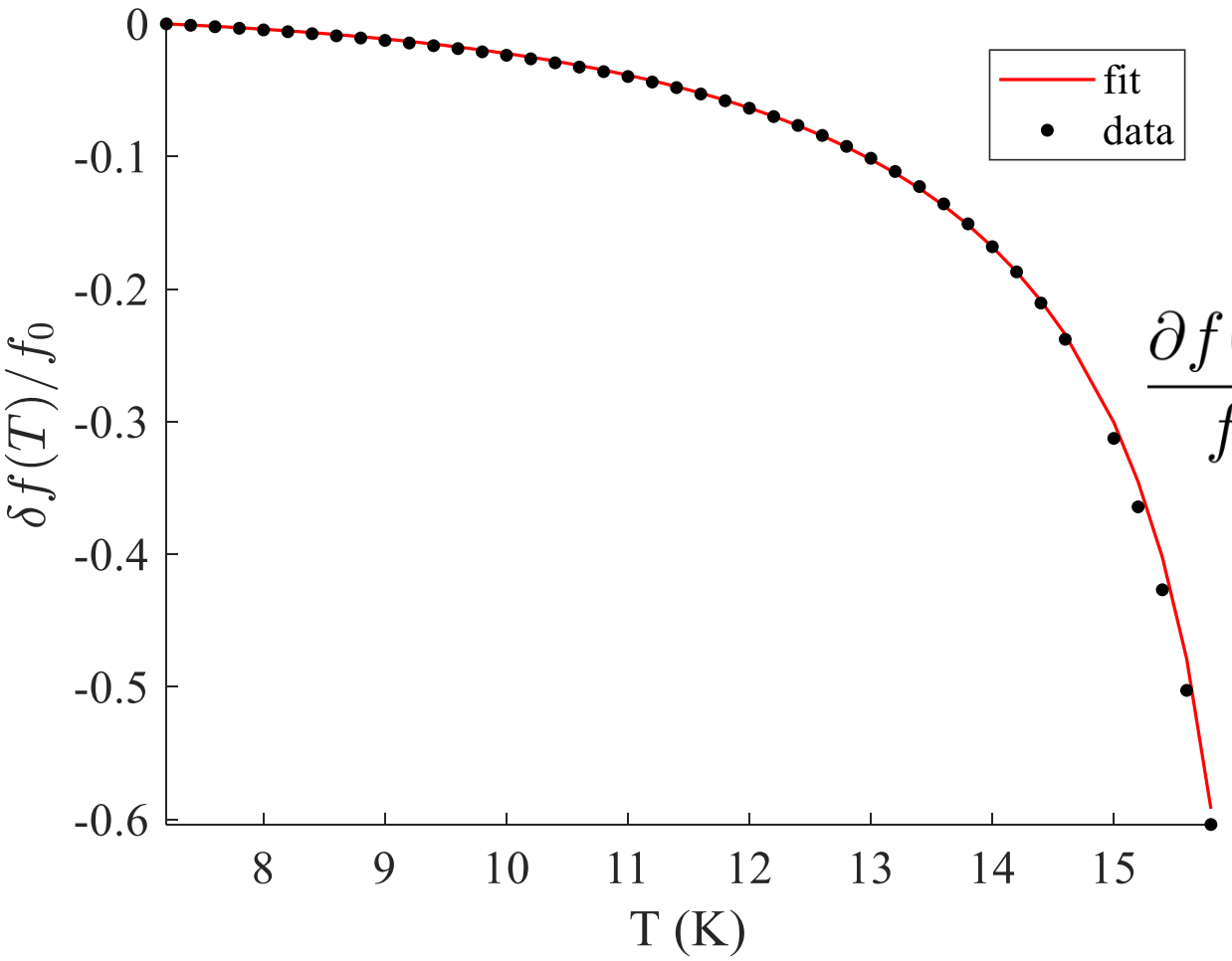

$$f = \frac{1}{2\pi\sqrt{LC}} = \frac{1}{2\pi\sqrt{(L_g + L_k(T))C}}$$

$$\frac{\partial f(T)}{f_0} = \frac{f(T) - f(7K)}{f(7K)} = \frac{\sqrt{L_g + L_k(7K)}}{\sqrt{L_g + L_k(T)}} - 1$$

$$L_k \approx \frac{\mu_0 \lambda^2(T)}{wt} \approx \frac{\mu_0}{wt} \frac{\lambda(0)^2}{1 - (\frac{T}{T_c})^4}$$

Fit gives $\lambda(0)$

Resonant frequency vs Temperature

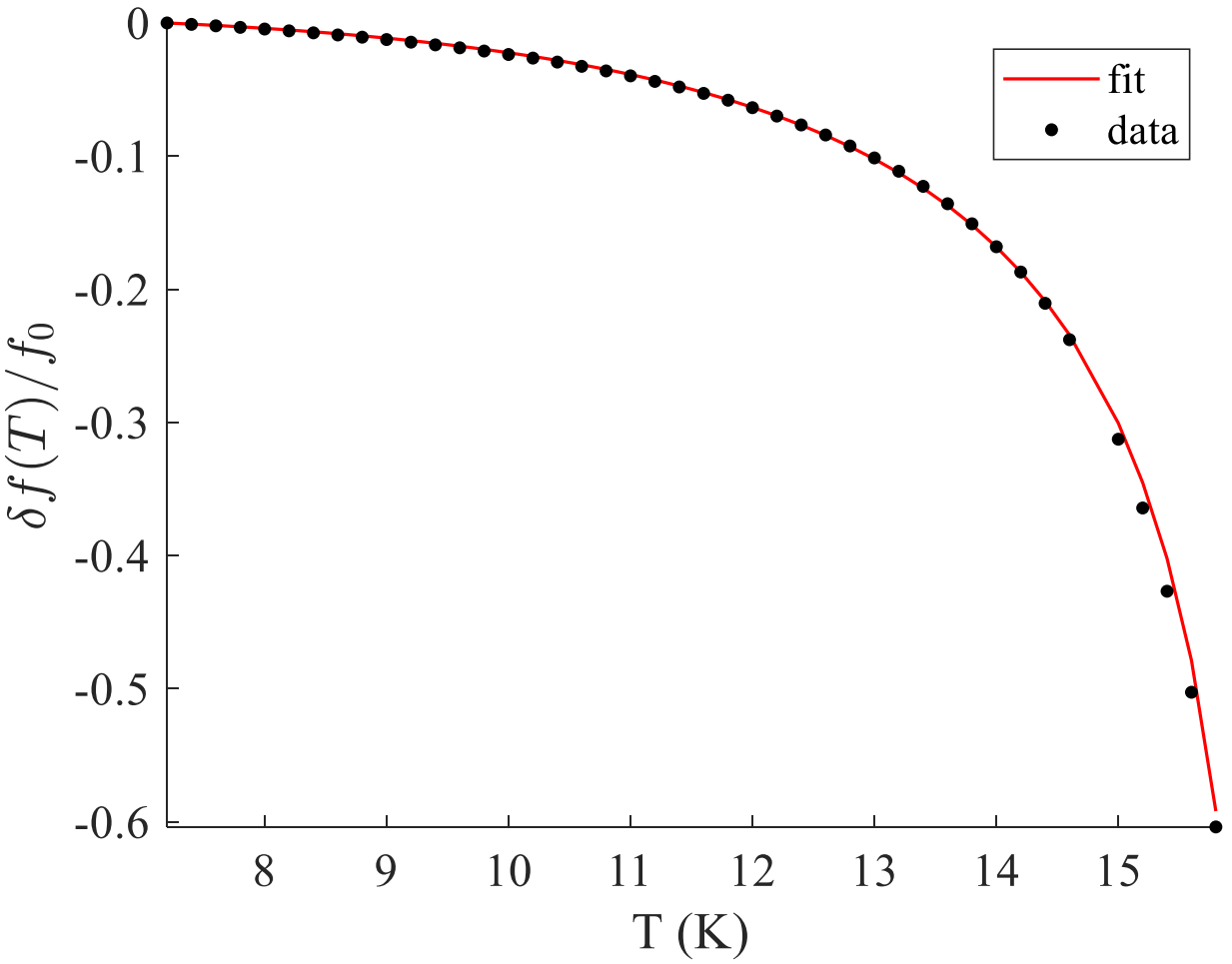

- $\lambda(0) = 353\ nm$
- Much larger than clean stoichiometric Nb_3Sn (90nm)
  - Nonstoichiometric inclusions
  - Grain boundaries

- Grain boundaries can facilitate a favorable condition for field penetration.

Field Alignment for the NLME measurements

- Eliminate contribution of the perpendicular field due to misalignment of the field orientation
- $B_{\perp}$ wraps around the edge and is enhanced
- Need to minimize the influence of fluxes by aligning the field parallel to the plane of the sample.

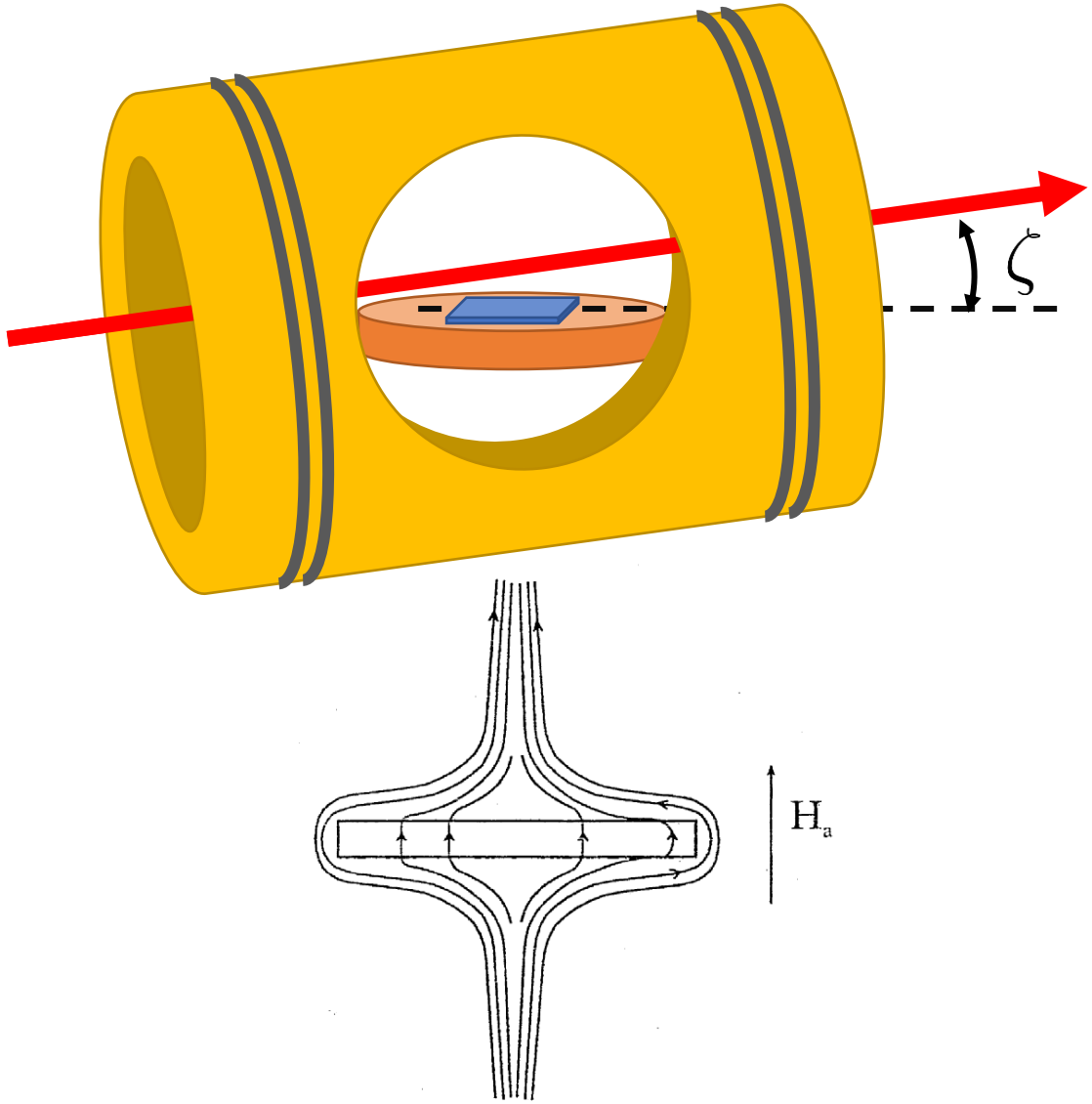

Steps for aligning the field

- Steps in aligning the field:
  1. Measure f_{0i} at $B = 0$
  2. Ramp the field to 60 mT and then back down to 0 mT
  3. Measure f_{0a} at $B = 0$ again
  4. Adjust the angle ζ until minimum of $(f_{0a} - f_{0i})/f_0$ is found

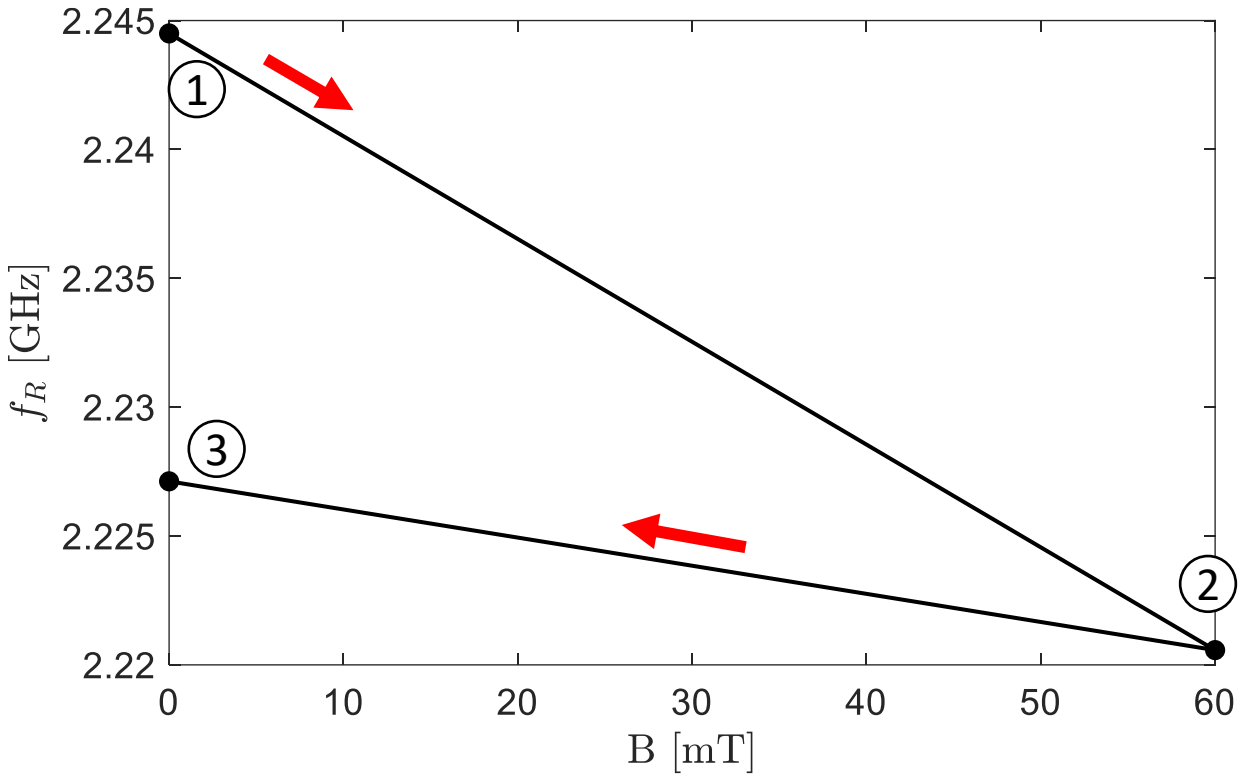

Field Alignment Results

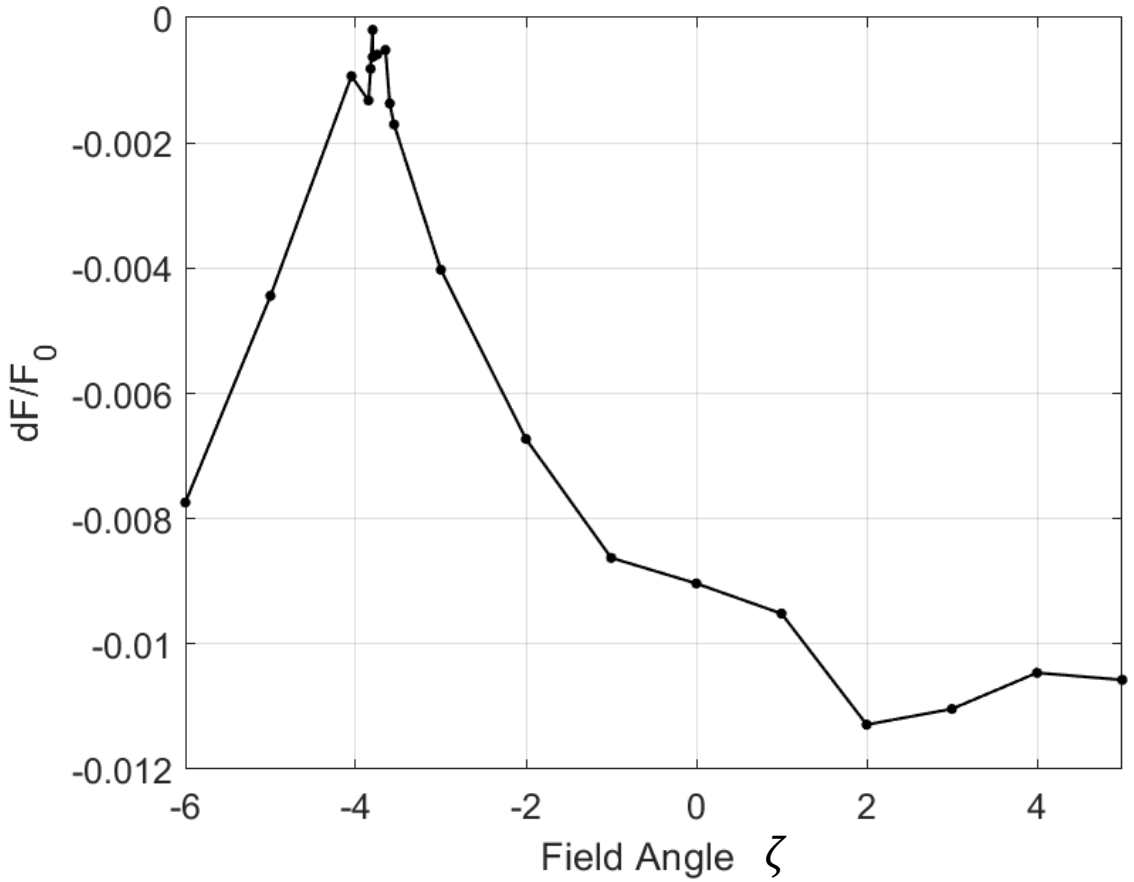

- Frequency shift is minimized at $\zeta = -3.8°$
- After aligning the field, measure $f_R(B)$ for temperature between 7K – 12K

Results of $f_r(B)$

- $f_r(B)$ decreases nearly linearly above 30-40mT
- Slope in B || z is almost twice as large as that of B || y

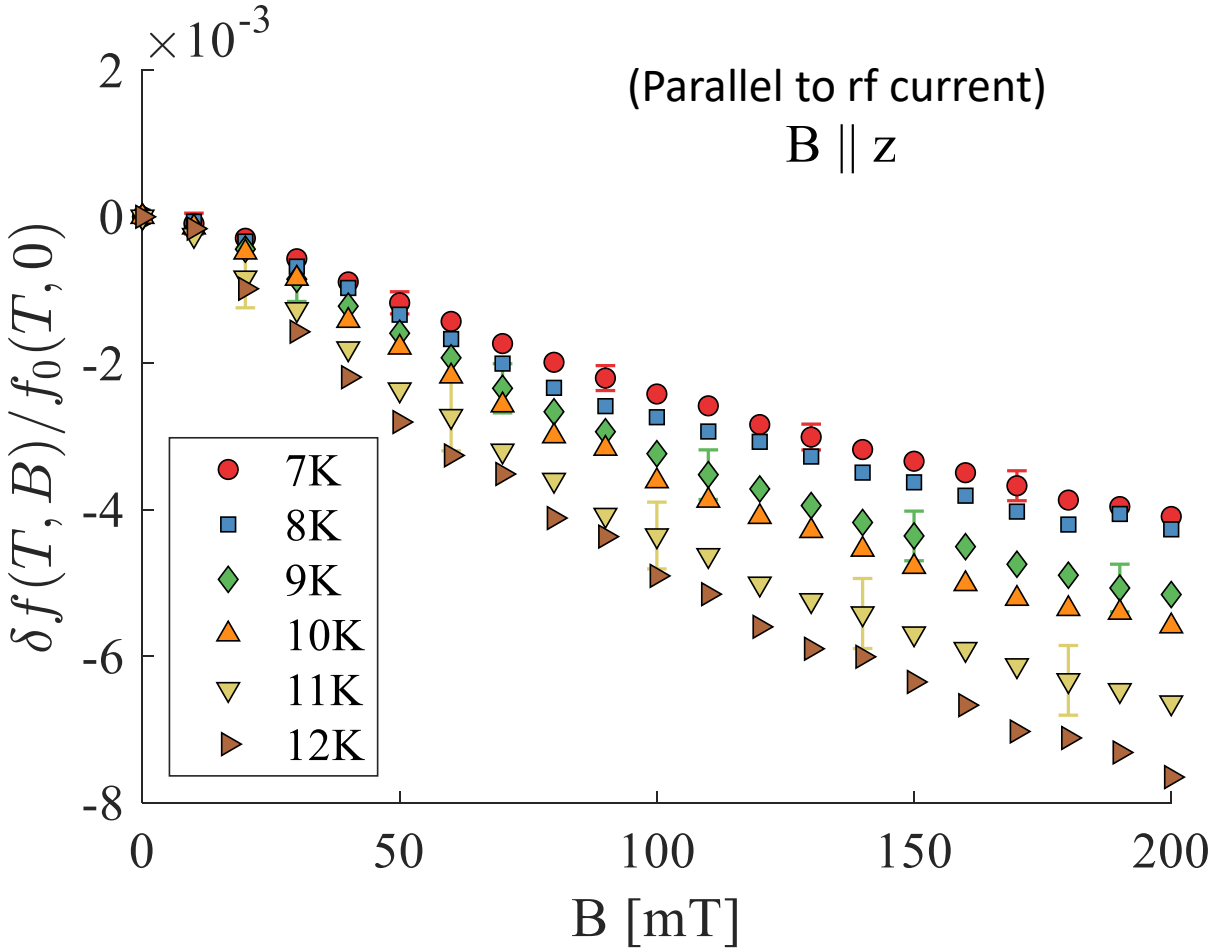

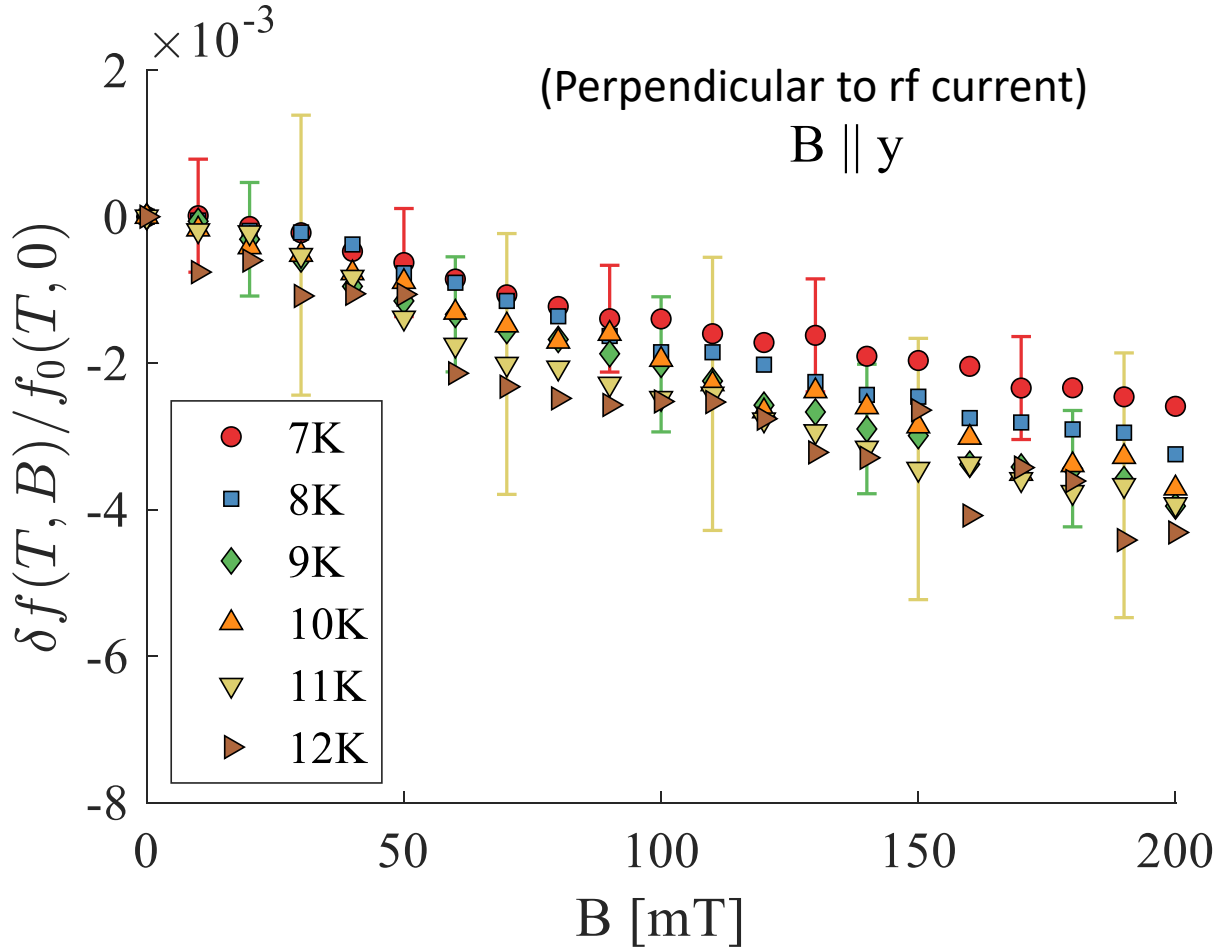

Contributions to NLME

- Pair breaking effect in which the current reduces n_s
- Weakly coupled grain boundaries and local non-stoichiometry on the surface cause an additional increase in λ

NLME Contribution from Pair Breaking

- The nonlinear current:

$$\mathbf{J} = -\frac{\mathbf{A}}{\mu_0 \lambda^2}\left(1 - \alpha(T)\frac{A^2}{A_c^2}\right)$$

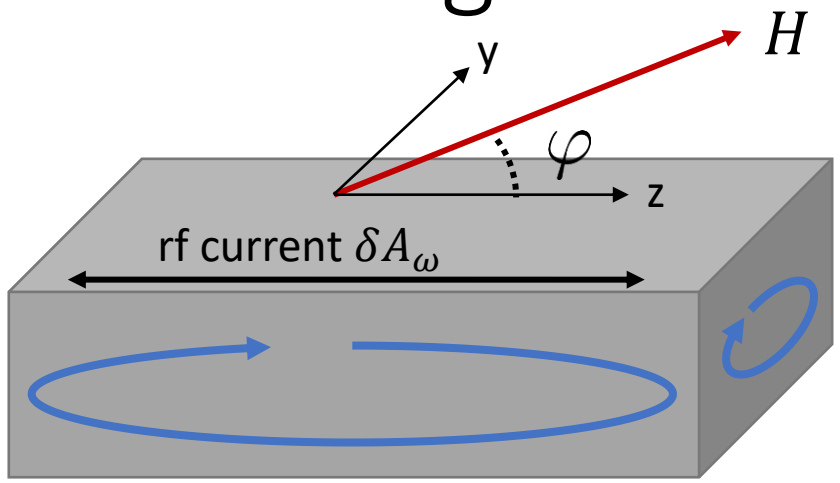

$$A_y = xB\cos\varphi \qquad A_z = xB\sin\varphi + \delta A_\omega$$

Only A_z component is coupled with the weak rf field

NLME Contribution from Pair Breaking

$$\lambda(B)^2 = \lambda^2(0)\left[1 + \frac{1}{3}\left(\frac{2\pi\xi tB}{\phi_0}\right)^2\left(\frac{1}{4} + \frac{2\sin^2\varphi}{4+\omega^2\tau^2}\right)\right]$$

$$\frac{\delta f}{f} = -\frac{1}{6}\left(\frac{\pi t\xi B}{\phi_0}\right)^2\left[1 + \frac{2\sin^2\varphi}{1+(\omega\tau/2)^2}\right]$$

- Pair-breaking NLME correction is quadratic in B
- $\sin^2\varphi$ angular dependence
  - Maximum when B is perpendicular to the rf current (B || y)

NLME Contribution from Pair Breaking

- $f_r(B)$ decreases nearly linearly above 30-40mT (not quadratic)
- Slope in B || z is almost twice as large as that of B || y (opposite)

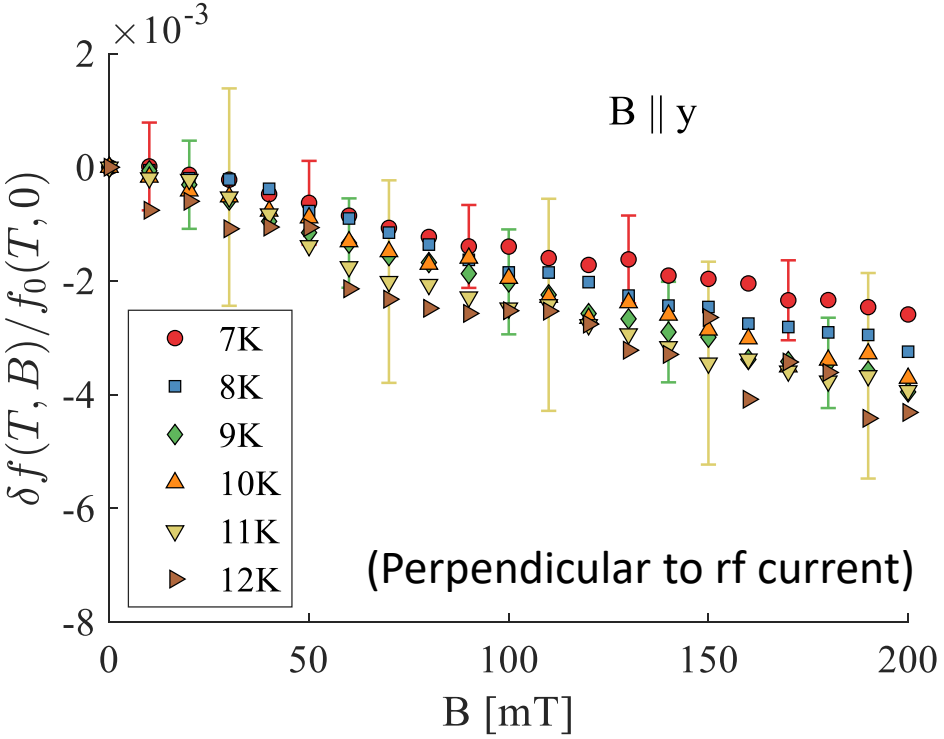

$$\frac{\delta f}{f} = -\frac{1}{6}\left(\frac{\pi t \xi B}{\phi_0}\right)^2 \left[1 + \frac{2\sin^2\varphi}{1+(\omega\tau/2)^2}\right]$$

At B = 100mT, $\frac{\delta f}{f} \approx 4 \times 10^{-4}$ for $\varphi = \frac{\pi}{2}$

This is much smaller than what we measured.

Grain Boundary Contribution

- A significant contribution to L_k can come from grain boundaries
- Sn depletion at grain boundaries acts as weak Josephson junctions.

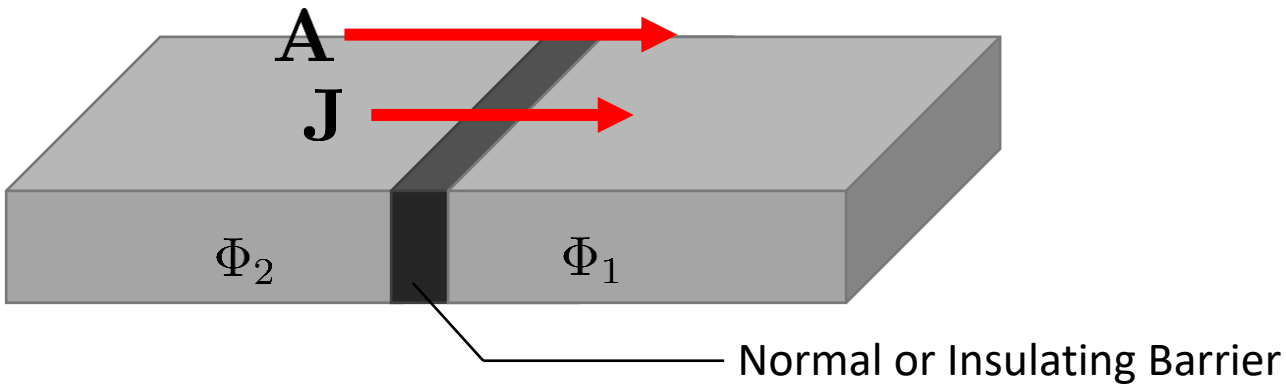

$$\mathbf{J} = J_c \sin\theta$$

J_c : Maximum current density across the barrier

$$\theta = \Phi_2 - \Phi_1 + \frac{2\pi}{\phi_0}\int \mathbf{A}\cdot d\mathbf{l}$$

Josephson Kinetic Inductance

- The grain boundary gives rise to additional Kinetic Inductance term

$$L_j = \frac{\phi_0}{2\pi I_c \cos\theta}$$

- The field dependence of $L_j(B)$ is determined by θ induced by the external field on the grain boundary.
- Low critical current can significantly increase L_j contribution

Grain Boundary Contributions

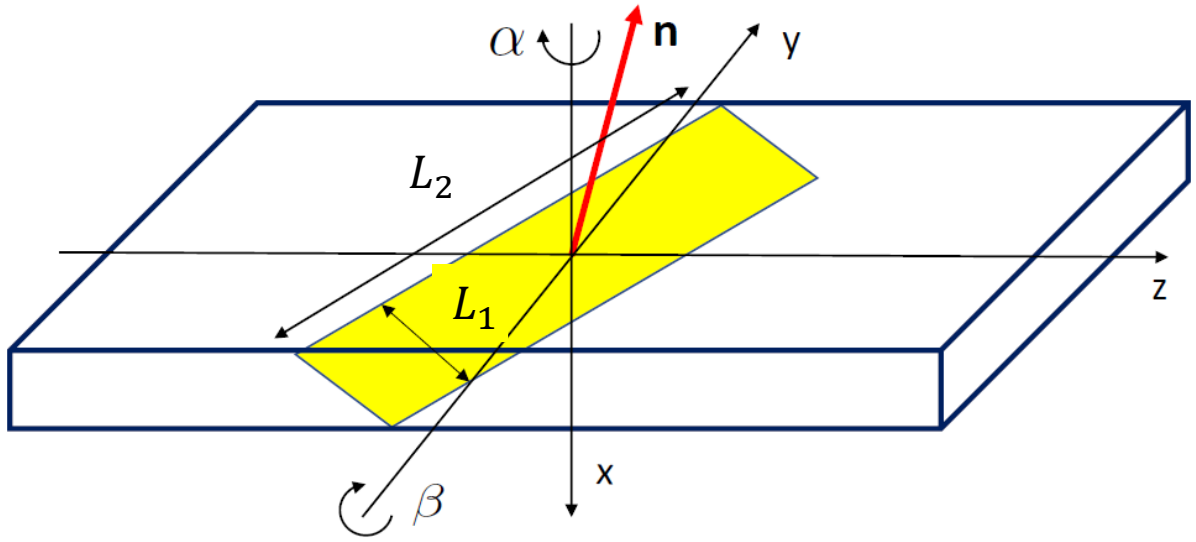

$L_1 \lesssim t \simeq 50\ nm$

$L_2 \sim 0.1 - 1\ \mu m$

- Calculate average $< \cos\theta(B) >$ for randomly distributed grain boundary
- $L_j(B) = \dfrac{\phi_0}{2\pi I_c <cos\theta(B)>}$

$$\frac{\delta f(B)}{f_0(0)} = \frac{\sqrt{L_g + L_j(0)}}{\sqrt{L_g + L_j(B)}} - 1$$

Numerical Calculation of GB Contributions

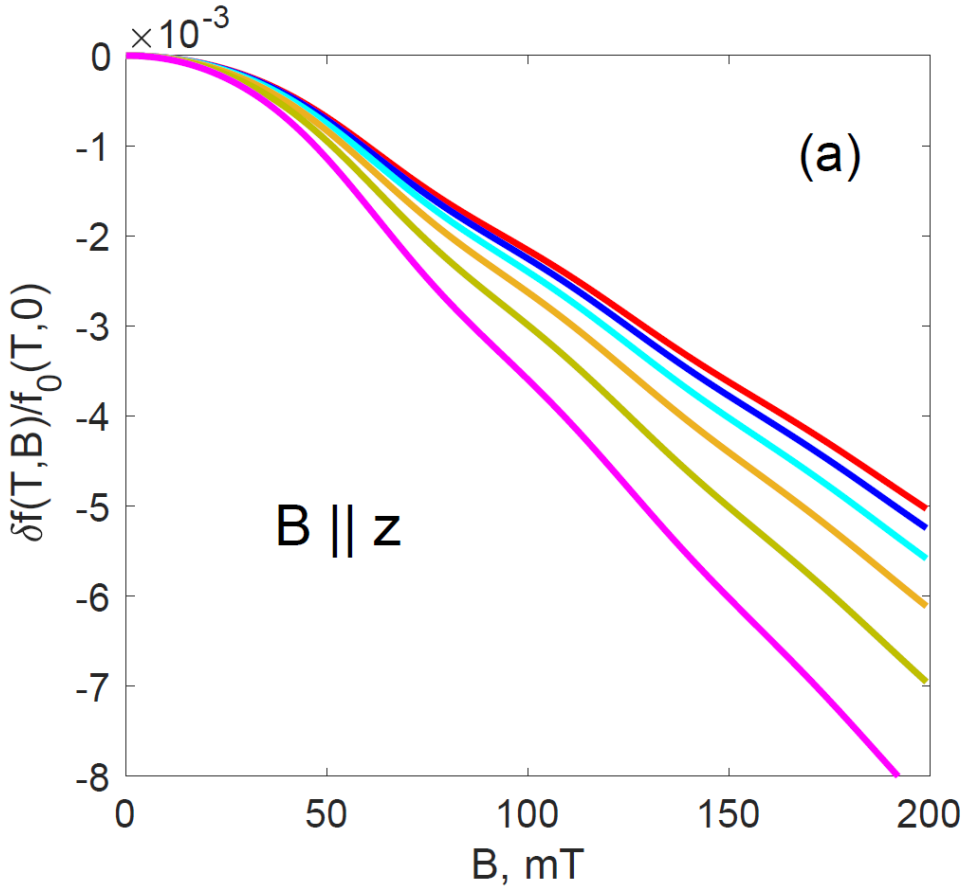

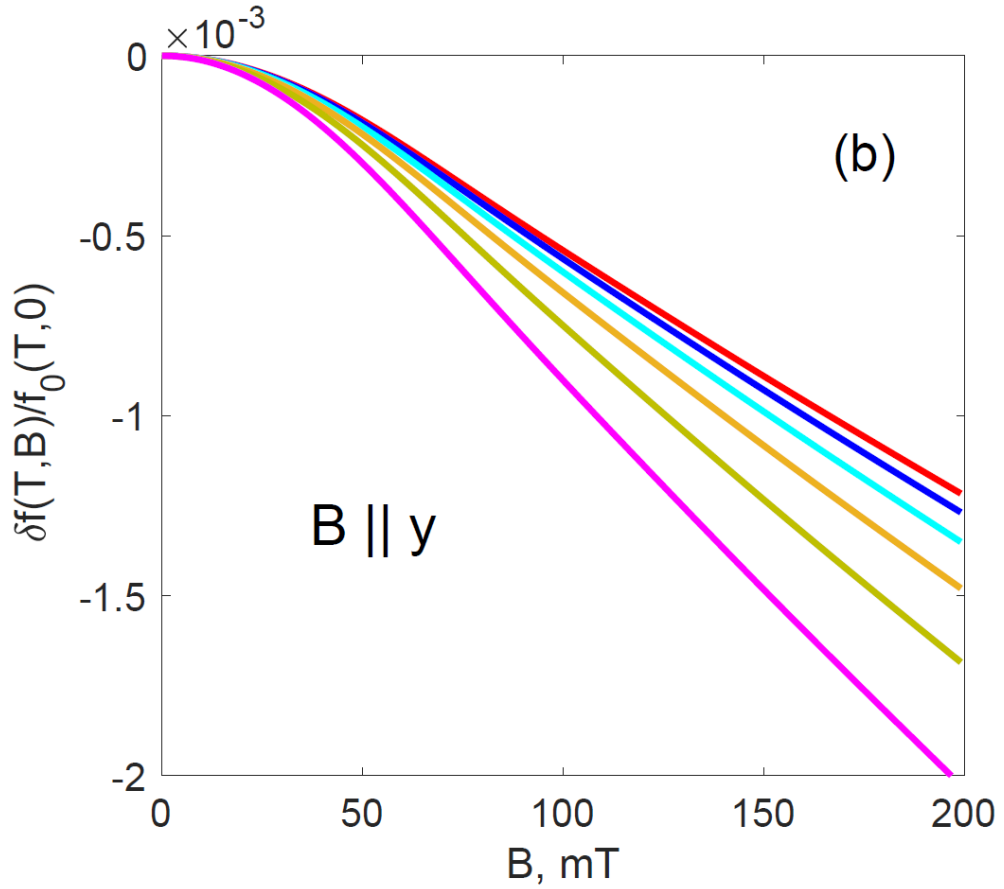

GB Contribution

- In general, both n_n and n_s can tunnel through the grain boundaries.
- Model the impedance across the grain boundary using a circuit model with $\langle L_j \rangle$ and R_{GB} in parallel

$$Z_j(B) = \left(\frac{1}{R_{GB}} + \frac{1}{i\omega \langle L_j \rangle} \right)^{-1}$$

$$R_j(B) \sim \frac{\omega^2}{wtl_2 R_{GB}} \langle L_j \rangle^2 \propto B^2$$

Conclusion

- The nonlinear Meissner effect on a thin Nb_3Sn film was studied in the cryogenic probe station.
- Aligning the field parallel to the film and using the thin film $t \ll \lambda$ extends the field onset of the penetration of the flux
- The results showed the linear dependence of the frequency with field, indicating that the weakly coupled grain boundaries can have a more significant contribution compared to the pair breaking Meissner current in a polycrystalline Nb_3Sn film.
- These results give an insight into nonlinear electrodynamic response to the field for a polycrystalline Nb_3Sn which could have additional field-dependent resistance in the SRF cavity.